Fundamental Performance Limits of Communications Systems Impaired by Impulse Noise

Riccardo Pighi, *Member, IEEE,* Michele Franceschini, *Member, IEEE,* Gianluigi Ferrari, *Member, IEEE,* and Riccardo Raheli, *Member, IEEE*

***Abstract*—In this paper, we investigate the ultimate performance limits, in terms of achievable *information rate* (IR), of communication systems impaired by impulse noise. We compare single carrier (SC) and multi-carrier (MC) transmission systems employing quadrature amplitude modulation (QAM) formats. More precisely, we consider SC schemes with coded modulations and MC systems based on orthogonal frequency division modulation (OFDM). For the MC schemes, we introduce a theoretically equivalent channel model which makes the computation of the IR feasible. This simple channel model will be referred to as *interleaved MC*. We show that, in the presence of impulse noise and except for systems operating at very high spectral efficiency, the IR of MC schemes is lower than that of SC schemes. More precisely, use of MC schemes may lead to an unavoidable fundamental loss with respect to SC schemes at typical coding rates, whereas MC schemes are to be preferred for very high coding rates or in uncoded systems. These results hold for additive white Gaussian noise (AWGN) and dispersive channels, either considering plain OFDM or MC schemes employing water-filling and bit-loading algorithms. In order to validate our theoretical results, we also obtain the bit error rate (BER) performance of SC and MC schemes through Monte Carlo simulations. A few trellis-coded modulation (TCM) and low-density parity-check (LDPC)-coded schemes are considered. The obtained SNR loss in the BER curves between the AWGN and impulse noise channels matches well with the corresponding IR gap.**

***Index Terms*—Impulse noise, information rate (IR), multitone modulation, orthogonal frequency division modulation (OFDM), trellis coded modulation (TCM), low-density parity check (LDPC) codes.**

I. Introduction

THE focus of this paper is on communications systems affected by impulse noise, which can be considered as a limiting factor in many scenarios, such as, for example, power line [1]–[3], digital subscriber line (DSL) [4], [5], and wireless communication systems [6]. Impulse noise typically originates from electromagnetic and electronic equipments and affects the transmission in the form of random bursts of relatively short duration and very high instantaneous power.

For narrowband applications, single carrier (SC) systems are typically adopted for their simplicity, usually with quadrature amplitude modulation (QAM), if high spectral efficiency is of interest. However, in broadband applications, frequency-selective channels and strong noise sources make multi-carrier (MC) modulation techniques, such as orthogonal frequency-division modulation (OFDM), an attractive solution for high-speed communications [7]–[12]. One of the original motivations for using multitone modulations was its improved robustness in impulse noise-limited communications [9]. In [13], the authors design optimized low-density parity-check (LDPC) codes for MC communication systems affected by impulse noise. The LDPC codewords are transmitted using bit-interleaved coded-modulation (BICM) techniques [14]. In [2], the performance of LDPC codes transmitted over Middleton Class A impulse noise channels [15]–[17] is analyzed using ad-hoc metrics in the LDPC decoding algorithm. In [18], the performance of LDPC codes for OFDM transmitted over Middleton Class A impulse noise channels is investigated, considering a proper time-domain (i.e., before OFDM demodulation) signal processing for detection and estimation of the impulse noise. The results in [18] show that the performance improvement brought by the use of time-domain processing may be significant. Although several works exist which analyze the bit error rate (BER) performance of practical coded systems, both SC and MC, the theoretical limits of communication systems impaired by impulse noise have received marginal attention. In particular, preliminary considerations on the capacity of impulse noise channels are presented in [19].

In this paper, we analyze the impact of impulse noise on the ultimate performance limits of SC and MC communication systems. In the first part of the paper, we study the theoretical limits of the considered schemes by means of computation and comparison of their information rates (IRs) [20]. IR-based analysis of communication schemes impaired by impulse noise provides engineers with an in-depth comprehension of the channel characteristics and a practical and valuable methodology for communication system design. As to MC systems, the theoretical analysis will be carried out (i) assuming uniform power and bit distribution over the available carriers, or (ii) applying water-filling and suitable bit loading algorithms [21],

Paper approved by C. L. Wang, the Editor for Equalization of the IEEE Communications Society. Manuscript received July 28, 2006; revised May 10, 2007, September 3, 2007, and December 27, 2007.

R. Pighi was with the Department of Information Engineering, University of Parma, Italy. He is now with Selta S.p.A., Italy (e-mail: r.pighi@selta.it).

M. Franceschini was with the Department of Information Engineering, University of Parma, Italy. He is now with IBM T. J. Watson Research Center, U.S.A.

G. Ferrari and R. Raheli are with the Department of Information Engineering, University of Parma, Italy.

This work appeared in part at the IEEE International Symposium on Power-Line Communications and its Applications, Orlando, FL, USA, March 2006.

Digital Object Identifier 10.1109/TCOMM.2009.0901.060440

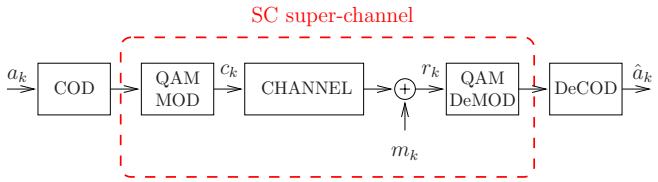

Fig. 1. SC communication system with AWGN, ISI and impulse noise.

[22]. Three different representative channels are considered: (i) additive white Gaussian noise (AWGN) channel with intersymbol interference (ISI), (ii) impulse noise channel with ISI, and (iii) *interleaved MC* channel with ISI. The last model allows one to evaluate the IR of standard MC systems, i.e., to investigate the ultimate performance limits of OFDM with channel coding distributed over the carriers. The theoretical results show that, while the introduction of additive impulse noise in a SC scheme with AWGN leads to negligible IR loss (even in the presence of a frequency selective channel), the impact of impulse noise on MC schemes may be significant at coding rates of practical interest. In the second part of this paper, we validate the information-theoretic results through a bit error rate performance analysis, based on Monte Carlo simulations, of several transmission schemes, both SC and MC. In particular, we consider (i) a trellis coded modulation (TCM) scheme [23]–[26] and (ii) an LDPC-coded [27], [28] QAM scheme. The obtained signal-to-noise ratio (SNR) loss in the BER curves between the AWGN and impulse noise channels matches well with the corresponding IR gap. This paper expands upon preliminary results presented in [29].

As a conclusion of our analysis, we show that the penalty which affects MC systems at coding rates of practical interest can be reduced using standard channel coding schemes complemented by suitable signal processing algorithms at the receiver side. In particular, proper time-domain processing, before MC demodulation, may be used to significantly reduce the degradation brought by the presence of impulse noise [18].

The paper outline is as follows. In Section II, we introduce the SC and interleaved MC schemes. In Section III, we evaluate the IR of the considered schemes, in order to investigate the ultimate theoretical performance limits in the presence of impulse noise. In Section IV, we evaluate, from a communication-theoretic perspective, the performance of the considered systems. Section V concludes the paper.

II. System and Channel Models

Since the focus of this paper is on the impact of impulse noise on standard SC and MC schemes, we consider, as references, either an *ideal* AWGN channel or a *dispersive* AWGN channel. For the sake of conciseness, the presence of impulse noise is taken into account through a simple Bernoulli-Gauss model [30]. However, the conclusions derived on the system performance are descriptive of the general effects of impulse noise and may be extended, e.g., to a Middleton Class A impulse noise model [15]–[17].

The SC communication scheme is depicted in Fig. 1: the QAM modulator and the corresponding demodulator are directly connected to the channel. The information symbol at the input of the encoder during the k-th signaling interval is denoted as a_k, c_k is the coded symbol transmitted over the channel through the QAM modulator, m_k is the realization of the overall noise process (including both impulse noise and AWGN), r_k is the discrete-time observable at the output of the channel, and $\hat{a}_k$ is the decoded information symbol at the output of the decoder. We assume that input information symbols are independent and identically distributed (i.i.d.). We refer to the cascade of blocks between the output of the encoder and the input of the decoder in a SC communication system as "SC super-channel."

The MC communication scheme is shown in Fig. 2: the QAM modulator is connected to the channel through a MC modulation block implementing an inverse discrete Fourier transform (IDFT). At the receiver side, the channel is connected to the QAM demodulator through a discrete Fourier transform (DFT) block. As in the SC scheme, a_k denotes the information symbol at the input of the encoder, c_k is the coded symbol at the input of the IDFT modulation block, η_n is the realization of the overall noise process (including both impulse noise and AWGN), y_n is the discrete-time observable at the input of the receiver, r_k is the observable at the output of the DFT demodulation block, and $\hat{a}_k$ is the estimated information symbol at the output of the decoder. In perfect analogy with the SC super-channel, we define as "MC super-channel" the cascade of all blocks between the output of the encoder and the input of the decoder in the MC communication system.

The evaluation of the IR of SC schemes is well-established [20], [31]–[34]. However, evaluating the IR of MC schemes is a more complicated computational problem. Since the MC modulation and demodulation blocks correspond to invertible vector functions (IDFT and DFT, respectively), the use of MC schemes does not modify the capacity of the overall channel [20]. Nevertheless, we will show that, in standard communication schemes with MC modulations, the implicit choice, made in code design/selection, of assuming independent samples conditionally on the transmitted sequence causes a significant IR loss at practical coding rates. This is reflected by the common MC scheme design practice, which typically adopts coding schemes originally derived for an AWGN channel (i.e., with conditionally independent observables) and sequentially distributes the coded symbols over the carriers.

In order to evaluate the impact of neglecting the conditional dependence of samples on the achievable IR in MC systems, we introduce a new channel model, referred to as *interleaved MC channel*. As shown in Fig. 3, the interleaved MC channel is a standard MC channel with, in addition, an ideal (infinite) interleaver (block Π) at the transmitter side and the corresponding deinterleaver (block Π^{-1}) at the receiver side. This interleaver eliminates the conditional dependence between the observables arising from the presence of impulse noise in the same OFDM block. In conventional communication systems, the use of interleaving is a well-known solution to reduce the channel memory, spread the errors, and make effective error correcting codes designed to correct random errors. This technique is also effective in coded multicarrier systems [35]. A key property of this scheme is that the channel seen by the modulator-demodulator pair is memoryless and this leads to a feasible and *exact* computation of the IR of the system. We

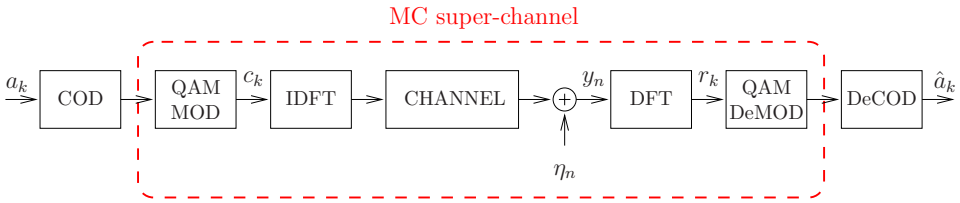

Fig. 2. MC communication system with AWGN, ISI and impulse noise.

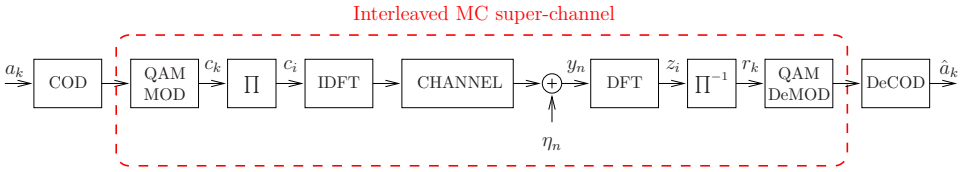

Fig. 3. *Interleaved* MC communication system (the ideal random interleaver is denoted as $\prod$) with AWGN, ISI and impulse noise.

will refer to all blocks between the output of the encoder and the input of the decoder as the "interleaved MC super-channel. We point out that the interleaved MC channel model justifies the assumption of conditional independence, for a given data sequence, between the observables at the output of the channel, and this allows to easily derive detection algorithms (see Section IV-A2). However, the obtained detection algorithms can be used also for a non-interleaved MC channel, as it is done in the numerical results (see Section IV-A3).

In order to evaluate the impact of the impulse noise, the following schemes will be compared: (i) a SC scheme with impulse noise and (ii) an interleaved MC scheme with impulse noise.

A. SC super-channel

As already described, the SC scheme affected by impulse noise is depicted in Fig. 1. The discrete-time observable at the output of a dispersive channel with AWGN and impulse noise can be expressed as follows:

$$r_k = \sum_{\ell=0}^{L} h_\ell c_{k-\ell} + m_k \tag{1}$$

where c_k is a code symbol belonging to a QAM constellation, $\{h_\ell\}_{\ell=0}^{L}$ are the coefficients of the discrete channel impulse response with length $L+1$, and m_k is the overall noise sample.

Assuming a Middleton Class A impulse noise model [15]–[17], the overall noise sample m_k has the following probability density function (PDF):

$$p(m_k) = \sum_{j=0}^{\infty} \frac{e^{-A}A^j}{j!} \frac{1}{2\pi\sigma_j^2} e^{-m_k^2/2\sigma_j^2} \tag{2}$$

with

$$\sigma_j^2 = \sigma^2 \left(\frac{j/A + \Gamma}{1+\Gamma} \right)$$

where A is the impulsive index, i.e., the product between the average number of impulses at the receiver in a time unit and their mean duration, $\Gamma = \sigma_w^2/\sigma_i^2$ is the Gaussian-to-Impulse noise power Ratio (GIR) with Gaussian noise power σ_w^2 and impulse noise power σ_i^2, and $\sigma^2 = \sigma_w^2 + \sigma_i^2$ is the total noise power. The sources of impulse noise are distributed according to a Poisson distribution with parameter A: one impulse noise source generates noise samples characterized by a Gaussian PDF with variance σ_i^2/A.

Another well-known model, widely used to represent the effects of impulse noise on communication systems, is the Bernoulli-Gauss model [30]. According to this model the overall noise sample m_k may be expressed as $m_k \triangleq w_k + i_k$, where w_k is a complex random variable with per-component power σ_w^2 and i_k is an impulse noise sample defined as [30]

$$i_k = b_k g_k \tag{3}$$

where b_k is a Bernoulli random variable (with values in $\{0,1\}$ and parameter $p = P\{b_k = 1\}$), and g_k is a complex white Gaussian random variable with zero mean and per-component variance σ_i^2. All of the above random variables are assumed independent with each other and with respect to the time index k. The Bernoulli-Gauss model is accurate for many natural impulsive noise sources, such as low-frequency atmospheric noise, man-made impulse noise, and noise sources occurring in urban and military radio networks [36], [37]. This model has also been used extensively to describe physical non-Gaussian noises [38]. In this case, the PDF $p(m_k)$ of the total channel noise m_k can be expressed as a mixture of Gaussian PDFs:

$$p(m_k) = (1-p)\mathcal{N}(m_k; 0, \sigma_w^2) + p\mathcal{N}(m_k; 0, \sigma_w^2 + \sigma_i^2) \tag{4}$$

where the notation $\mathcal{N}(m; \eta, \sigma^2) \triangleq (1/2\pi\sigma^2)\exp\{-|m-\eta|^2/2\sigma^2\}$ denotes a circularly symmetric complex Gaussian PDF with mean η and per-component variance σ^2. The mixture noise density model (4) represents the impulse noise as a sequence of random-amplitude and randomly occurring narrow pulses in a background Gaussian noise [38].

Note that the sum in (2) for sufficiently low values of the parameter A may be well approximated considering its first few terms, i.e., only the very first terms in (2) are significant. This observation implies that, in many practical scenarios, the Bernoulli-Gauss model may be considered as a good approximation for the canonical Class A interference model. In fact, the statistical descriptions of the two noise models coincide if the summation in (2) is limited to its first two

terms. This approximation is accurate if A is sufficiently small. As an example, assuming $A = 0.01$ [39], [40], the probability associated to the third term in (2), i.e., $e^{-A}A^2/2$, is two orders of magnitude smaller than the value of the first term e^{-A}. Based on these observations, in the remainder of this paper the impulse noise will be modeled according to the Bernoulli-Gauss distribution.

B. Interleaved MC super-channel

The interleaved MC scheme with Bernoulli-Gauss impulse noise is depicted in Fig. 3. We now characterize the input-output relationship of the interleaved MC super-channel.

A MC signal is generated by taking the IDFT of a block of (interleaved) symbols $\{c_i\}$ belonging to a QAM constellation. The useful part of each OFDM symbol has a duration of T seconds and is preceded by a cyclic prefix that is longer than the channel impulse response: in this way, the interference between adjacent symbols is eliminated. Assuming N modulated subcarriers, the observables at the output of the dispersive channel with Bernoulli-Gauss impulse noise at time n during the v-th OFDM symbol period may be expressed as follows:

$$y_{n+vN} = s_{n+vN} + \eta_n = s_{n+vN} + w_n + i_n \quad 0 \le n \le N-1$$

in which η_n is the overall noise sample, w_n is a sample of AWGN, i_n is the Bernoulli-Gauss impulse noise sample defined in (3), and s_{n+vN} is the useful part of the signal carrying the interleaved QAM coded symbol sequence $\{c_i\}$. For N sufficiently large, the term s_{n+vN} can be expressed as [41]

$$s_{n+vN} = \frac{1}{\sqrt{N}} \sum_{i=0}^{N-1} c_{i+vN} H_i \, e^{\jmath 2\pi n f_i T} \qquad 0 \le n \le N-1$$

where $f_i \triangleq i/T$ is the frequency of the i-th subcarrier and H_i is the channel response at frequency f_i. The observable at the output of the DFT demodulation block of the v-th symbol can be expressed as follows:

$$z_{i+vN} = \frac{1}{\sqrt{N}} \sum_{n=0}^{N-1} y_{n+vN} \, e^{-\jmath 2\pi n i/N} = H_i c_{i+vN} + W_i + I_i$$

where the last equality is due to the linearity of the DFT, W_i is a sample of the DFT of $\{w_n\}$, i.e., an i.i.d. thermal noise sample with variance σ_w^2 per component, and I_i is defined as the DFT of $\{i_n\}$, i.e.:

$$I_i \triangleq \frac{1}{\sqrt{N}} \sum_{n=0}^{N-1} i_n \, e^{-\jmath 2\pi n i/N} \qquad 0 \le n \le N-1 \, .$$

The PDF of the total noise sample at the output of the DFT, i.e., $\Omega_i = W_i + I_i$, can be expressed as [30]

$$p(\Omega_i) = \sum_{\ell=0}^{N} \binom{N}{\ell} p^{\ell} (1-p)^{N-\ell} \mathcal{N}(\Omega_i; 0, \sigma_\Omega^2[\ell]) \qquad (5)$$

where

$$\sigma_\Omega^2[\ell] \triangleq \sigma_w^2 + \ell \frac{\sigma_i^2}{N} \, . \qquad (6)$$

For the sake of clarity, it should be pointed out that (5) corresponds to the PDF of the overall noise at the output of the DFT block when the impulse noise has a Bernoulli-Gauss distribution. In the more general case of Middleton Class A impulse noise model, it is possible to express the PDF of the overall noise using a multinomial combination of Gaussian PDFs. For ease of illustration, we do not pursue this extension here.

As observed in the previous section, we ideally assume that, at the transmitter, an infinite random interleaver is inserted between the QAM modulator and the IDFT block and, at the receiver, the corresponding ideal deinterleaver is inserted between the DFT block and the QAM demodulator. As a consequence, the discrete-time observable at the output of this channel can be expressed as

$$r_{k+vN} = H_k c_{k+vN} + m_k \, .$$

The above assumption allows one to conclude that consecutive QAM coded symbols are affected, at the receiver, by i.i.d. noise samples $\{m_k\}$ with PDF given by (5). Consequently, it is feasible to obtain *exact* information-theoretic results and *practical* detection/decoding algorithms.

III. Information-Theoretic Performance Analysis: Information Rate

The IR between the sequence of uncoded input symbols $\{a_k\}$ and the output sequence $\{r_k\}$ of a general dispersive channel can be expressed as [20]

$$I(\mathcal{A}; \mathcal{R}) = h(\mathcal{R}) - h(\mathcal{R}|\mathcal{A}) \qquad (7)$$

where $h(\mathcal{R})$ and $h(\mathcal{R}|\mathcal{A})$ are the differential and conditional differential entropy rates of the sequence $\{r_k\}$ given $\{a_k\}$, respectively. In an AWGN scenario, the conditional differential entropy rate $h(\mathcal{R}|\mathcal{A})$ has the well-known expression $(1/2)\log(2\pi e \, \sigma_w^2)$ [20]. Due to the presence of impulse noise, however, $h(\mathcal{R}|\mathcal{A})$ must be evaluated by numerical simulations. In [31]–[34], a simulation-based method to compute the IRs of channels with memory, e.g., intersymbol interference (ISI) channels with AWGN, is presented. We now apply this method to communication scenarios affected by impulse noise.

Since $\{r_k\}$ is a stationary ergodic process, the Shannon-McMillan-Breiman theorem holds [20], [42] and it is possible to evaluate $h(\mathcal{R})$ using a reasonably long information sequence by means of proper simulations. As a consequence, the differential entropy rate of the sequence[1] $\boldsymbol{r}_1^n$ can be expressed as

$$\begin{aligned} h(\mathcal{R}) &= \lim_{n\to\infty} \frac{1}{n} h(\boldsymbol{r}_1^n) \\ &= -\lim_{n\to\infty} \frac{1}{n} \mathbb{E}\left[\log(p(\boldsymbol{r}_1^n))\right] \\ &= -\lim_{n\to\infty} \frac{1}{n} \log\left[p(\boldsymbol{r}_1^n)\right] \end{aligned} \qquad (8)$$

where $p(\boldsymbol{r}_1^n)$ is the PDF of the channel output sequence $\boldsymbol{r}_1^n$. Moreover, the joint stationarity and ergodicity of $\{r_k\}$ and $\{a_k\}$ allows one to express the conditional differential entropy

[1]Note that $\boldsymbol{r}_{k_1}^{k_2}$ is a shorthand notation for the vector collecting signal observations from time epoch k_1 to k_2.

of the sequence $\boldsymbol{r}_1^n$ as

$$\begin{aligned} h(\mathcal{R}|\mathcal{A}) &= \lim_{n\to\infty}\frac{1}{n}h(\boldsymbol{r}_1^n|\boldsymbol{a}_1^n) \\ &= -\lim_{n\to\infty}\frac{1}{n}\mathbb{E}\left[\log(p(\boldsymbol{r}_1^n|\boldsymbol{a}_1^n))\right] \\ &= -\lim_{n\to\infty}\frac{1}{n}\log[p(\boldsymbol{r}_1^n|\boldsymbol{a}_1^n)] \\ &= -\lim_{n\to\infty}\frac{1}{n}\log[p(\boldsymbol{m}_1^n|\boldsymbol{a}_1^n)] \\ &= -\lim_{n\to\infty}\frac{1}{n}\log[p(\boldsymbol{m}_1^n)] \\ &= -\lim_{n\to\infty}\frac{1}{n}\sum_{i=1}^{n}\log p(m_i)\,. \end{aligned} \tag{9}$$

Given the memoryless nature of the overall additive noise, the conditional PDF $p(\boldsymbol{r}_1^n|\boldsymbol{a}_1^n)$ embedded in (9) can be easily expressed using (4) and (5) for both SC or MC schemes.

We then address to the evaluation of the differential entropy rate $h(\mathcal{R})$ for SC and MC schemes. As to SC schemes, in [31]–[34] it is shown how the forward recursion of the BCJR algorithm [43] can be used to compute $p(\boldsymbol{r}_1^n)$ by defining a trellis diagram for the overall dispersive discrete-time channel, with an appropriate state ζ_k, at time epoch k, defined as $\zeta_k \triangleq (a_{k-1}, a_{k-2}, \ldots, a_{k-L})$, where L is the channel memory (in terms of symbol intervals). With these definitions, one can evaluate the PDF of $\boldsymbol{r}_1^k$ as

$$p(\boldsymbol{r}_1^k) = \sum_{\zeta_k} p(\boldsymbol{r}_1^k|\zeta_k)P(\zeta_k) = \sum_{\zeta_k}\mu(\zeta_k)$$

where the "metric" $\mu(\zeta_k)$ is defined as[2]

$$\mu(\zeta_k) \triangleq p(\boldsymbol{r}_1^k|\zeta_k)P(\zeta_k)\,. \tag{10}$$

Marginalizing over the previous states and using the chain factorization rule, one can rewrite (10) as [31]–[34]

$$\begin{aligned} \mu(\zeta_k) &= p(\boldsymbol{r}_1^k|\zeta_k)P(\zeta_k) \\ &= \sum_{\zeta_{k-1}} p(r_k|\zeta_k,\zeta_{k-1})P(\zeta_k|\zeta_{k-1})\mu(\zeta_{k-1}) \end{aligned} \tag{11}$$

where we have introduced $\mu(\zeta_{k-1}) = p(\boldsymbol{r}_1^{k-1}|\zeta_{k-1})P(\zeta_{k-1})$ and exploited the independence between the observables. Note that the metrics at time epoch 0 are initialized according to a uniform distribution, i.e., $\mu(\zeta_0) = 1/(\log_2 Q)^L$ with Q being the cardinality of the QAM constellation and $(\log_2 Q)^L$ being the number of trellis states. Given the memoryless nature of the noise, the PDF $p(r_k|\zeta_k,\zeta_{k-1})$ in (11) can be expressed as

$$\begin{aligned} p(r_k|\zeta_k,\zeta_{k-1}) &= (1-p)\mathcal{N}\left(r_k;\sum_{\ell=0}^{L}h_\ell a_{k-\ell},\sigma_w^2\right) \\ &\quad + p\mathcal{N}\left(r_k;\sum_{\ell=0}^{L}h_\ell a_{k-\ell},\sigma_w^2+\sigma_i^2\right) \end{aligned} \tag{12}$$

As to MC schemes, the independence between the observables allows one to factor (8) as

$$\begin{aligned} h(\mathcal{R}) &= -\lim_{n\to\infty}\frac{1}{n}\log\left[p(\boldsymbol{r}_1^n)\right] \\ &= -\lim_{n\to\infty}\frac{1}{nN}\sum_{v=0}^{n-1}\sum_{k=0}^{N-1}\log p(r_{k+vN}) \end{aligned}$$

[2]In a detection-theoretic sense, $\log\mu(\zeta_k)$ is a metric.

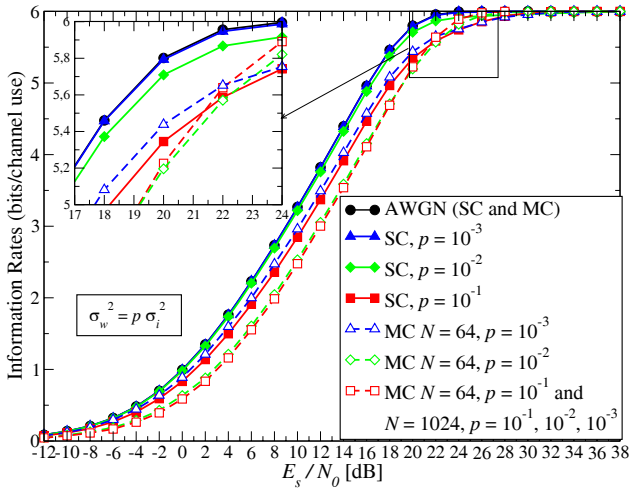

Fig. 4. IR for 64 QAM schemes, both SC and interleaved MC, with impulse noise. In each case, various values of the parameter p of the Bernoulli distribution for the impulse noise are considered. The variances of AWGN and impulse noise are equal for all values of p, i.e., $\sigma_w^2 = p\,\sigma_i^2$. The number of MC sub-channels is set to $N = 64$ or $N = 1024$.

where

$$\begin{aligned} &p(r_{k+vN}) \\ &= \sum_{\ell=0}^{N}\binom{N}{\ell}p^\ell(1-p)^{N-\ell}\mathcal{N}(r_{k+vN};H_k a_{k+vN},\sigma_\Omega^2[\ell]). \end{aligned} \tag{13}$$

A. Numerical Results

In Fig. 4, the IR of SC and interleaved MC schemes with 64 QAM, Bernoulli-Gauss impulse noise, and a non-dispersive channel is shown. For the interleaved MC channel, the number N of sub-channels is set to either 64 or 1024, with uniform power and bit distribution over each subcarriers. The IR is shown as a function of the SNR E_s/N_0, where E_s is the average received symbol energy and N_0 is the one-sided AWGN power spectral density. The Bernoulli parameter p takes on values in the representative set $\{10^{-1}, 10^{-2}, 10^{-3}\}$. The variance of the impulse noise is such that the average powers of thermal and impulse noise are equal, i.e., $\sigma_w^2 = p\,\sigma_i^2$. This particular choice leads to an intuitive comparison of the relative effects of both types of noise. Note that, in order to focus our attention only on the impact of impulse noise, the computation of the IR has been carried out using (i) Monte Carlo simulations for the evaluation of the limits in (8) and (9) and (ii) assuming a non-dispersive channel, i.e., $L = 0$ and $H_i = 1$, for $i = 0, \ldots, N-1$. The number of transmitted symbols is set to 10^7, which guarantees good numerical accuracy. In order to avoid numerical problems, the evaluation of (12) and (13) has been performed in the logarithmic domain.

In the SC case, the introduction of impulse noise causes an SNR loss, with respect to the AWGN channel (curve with $p = 0$). For example, at a representative IR value of 5.5 bits per channel use, the loss equals approximately 3 dB at $p = 10^{-1}$, 0.56 dB at $p = 10^{-2}$, and negligible at $p = 10^{-3}$. As expected, when $p = 10^{-1}$ a large fraction of the received signal samples are affected by a strong noise, and this leads to the SNR loss shown in Fig. 4. On the other hand, for values of p lower than

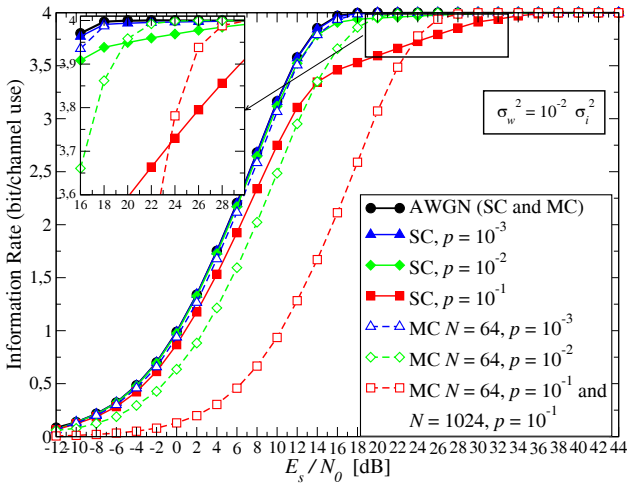

Fig. 5. IR for 16 QAM schemes, both SC and interleaved MC, with impulse noise. In each case, various values of the parameter p of the Bernoulli distribution for the impulse noise are considered. The variances of AWGN and impulse noise are equal for $p = 10^{-2}$ only, i.e., $\sigma_w^2 = 10^{-2}\,\sigma_i^2$. The number of MC sub-channels is set to $N = 64$ or $N = 1024$.

10^{-2}, the SNR loss is negligible. As to the interleaved MC case with $N = 64$, the SNR loss, with respect to the AWGN channel, is 3 dB at $p = 10^{-1}$, 3.3 dB at $p = 10^{-2}$, and 2.23 dB at $p = 10^{-3}$ at an IR value of 5.5 bits per channel use, respectively. Finally, for the interleaved MC scheme with $N = 1024$, the IR curves obtained with $p = 10^{-1}, p = 10^{-2}$, and $p = 10^{-3}$ overlap with that obtained with $N = 64$ and $p = 10^{-1}$. From Fig. 4 one can conclude that, for a fixed value of the Bernoulli parameter p and excluding very high IR values, the SNR penalty incurred by the interleaved MC scheme is higher than that incurred by the SC scheme. Moreover, this penalty increases with the number of subcarriers N for a given value of the Bernoulli parameter p. Note that at very high values of IR a MC scheme may outperform a SC scheme. We will discuss this aspect in some depth in the comment of the following figure.

In Fig. 5, the IR of SC and interleaved MC schemes with Bernoulli-Gauss impulse noise and a non-dispersive channel is shown for 16 QAM. For the interleaved MC channel, the number N of carriers is set to either 64 or 1024, and we assume uniform power and bit distribution over each subcarriers. Unlike the previous figure, the variance of the impulse noise is now such that the average powers of AWGN and impulse noise are equal *only* when $p = 10^{-2}$, i.e., $\sigma_w^2 = 10^{-2}\,\sigma_i^2$. Therefore, the case with $p = 10^{-2}$ corresponds to that considered in the previous figure (Fig. 4), except for the modulation order. For $p = 10^{-1}$ and $p = 10^{-3}$, the power of the impulse noise is higher and lower than that of the AWGN, respectively.

As one can observe from the results in Fig. 5, for $p = 10^{-1}$, the behavior of the IR for both SC and interleaved MC schemes differs from that in Fig. 4. More precisely, in the SC case, once an IR curve reaches a critical value (in terms of bits/channel use), its slope reduces significantly and the IR increases almost linearly. In other words, in the presence of frequent impulse noise bursts, the SNR required to achieve the maximum possible channel utilization (i.e., an IR close to 4 bits/channel use) is significantly higher than that necessary in a scenario where the impulse noise bursts are rare. The different slopes of these curves partitions the graph in two different regions, corresponding to AWGN-limited (low SNR) and impulse noise-limited (high SNR) regions, respectively. The critical IR value is obtained in correspondence to the border between these regions. In particular, one might expect that, in correspondence to this border, the impulse noise is strong and leads, therefore, to a complete erasure of the transmitted symbol. The IR for M QAM transmitted through a discrete M-ary erasure channel with erasure probability p is given by the following expression [20]:

$$\begin{aligned} I_{\mathrm{E}}(\mathcal{A};\mathcal{R}) &= H(\mathcal{A}) - H(\mathcal{A}|\mathcal{R}) \\ &= \log_2 M - p\log_2 M = (1-p)\log_2 M\,. \end{aligned}$$

This expression is based on the assumption that when there is an "erasure," any possible M QAM symbol could have equally likely been transmitted. As a consequence, in the 16 QAM case, the expected IR critical value, in correspondence to which the IR slope changes[3], is approximately equal to $4(1-p)$. This is substantially confirmed by the results in Fig. 5.

In the MC case with $N = 64$ (and $N = 1024$) in Fig. 5, on the other hand, the impact of the impulse noise consists, as long as $Np \gg 1$, of a translation of the IR curve, i.e., the impulse noise causes an SNR penalty. In particular, for $p = 10^{-1}$ the penalty is about 10 dB, and this is consistent with the average noise power increase due to the impulse noise for $\sigma_w^2 = 10^{-2}\sigma_i^2$. Note that, as in Fig. 4, for the interleaved MC scheme with $N = 1024$, the IR curve obtained with $p = 10^{-1}$ overlaps with the IR obtained with $N = 64$ and $p = 10^{-1}$, since in both cases $Np \gg 1$.

A careful inspection of the results in Fig. 5 shows that MC schemes may outperform, in terms of IR, SC schemes only at very high spectral efficiency, as shown in the zoom box within Fig. 5. This finding reflects the common idea that MC schemes are more robust to impulse noise than SC schemes. However, our results show that this is only true at high spectral efficiency, e.g., in the typical operating region of uncoded schemes. The results presented in Fig. 5 can also be interpreted as the theoretic counterpart of the symbol error rate (SER) analysis carried out in [30] for uncoded schemes in the presence of impulse noise, where it was shown that MC uncoded systems present a better SER performance with respect to SC uncoded schemes. We point out, however, that practical communication systems tend to employ channel coding, lowering the spectral efficiency to values where the SNR loss incurred by MC schemes may be significant. A careful selection of the proper coding rate should take into account these IR-based findings.

In Fig. 6, the IR of SC and interleaved MC schemes is shown, as a function of the SNR, in a scenario with Bernoulli-Gauss impulse noise, 16 QAM, and in the presence of a dispersive channel with impulse response $h(t) = [\delta(t) + 2\delta(t-T) + \delta(t-2T)]/\sqrt{6}$. As in Fig. 5, we assume that $\sigma_w^2 = 10^{-2}\,\sigma_i^2$. In the MC case, the number N of subcarriers is set to 64 and uniform power and bit distribution over each subcarriers is considered. For example, at a representative IR

[3]For $p = 10^{-2}$ and $p = 10^{-3}$, only a vestigial slope change can be perceived.

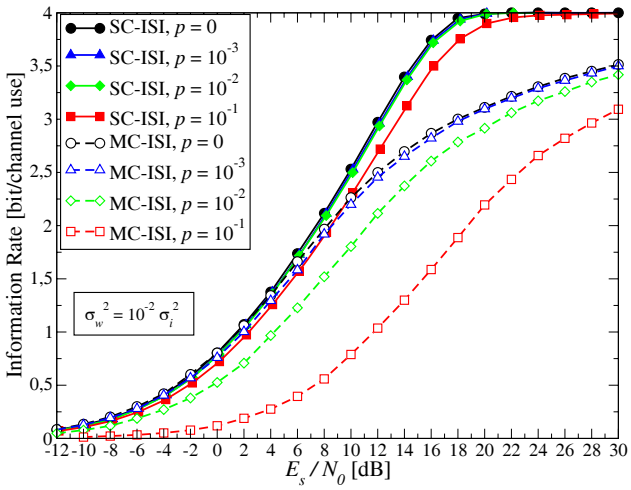

Fig. 6. IR for 16 QAM schemes, both SC and interleaved MC, with impulse noise and a time-dispersive channel. In each case, various values of the parameter p of the Bernoulli distribution for the impulse noise are considered. The variances of AWGN and impulse noise are equal for $p = 10^{-2}$ only, i.e., $\sigma_w^2 = 10^{-2}\,\sigma_i^2$. The number of MC sub-channels is set to $N = 64$.

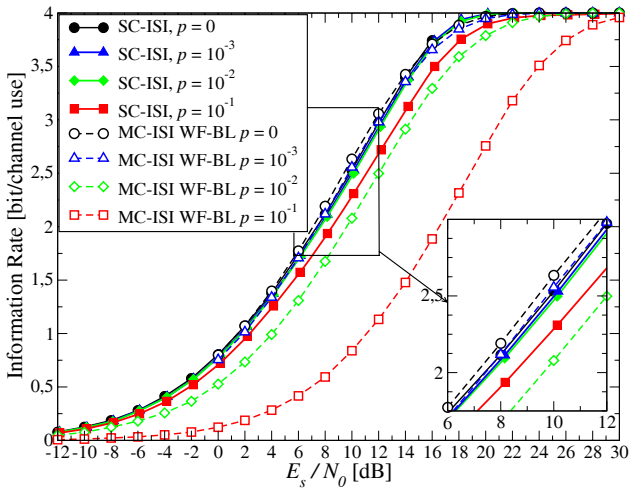

Fig. 7. IR for a 16 QAM SC scheme and an interleaved MC with water-filling and bit-loading (WF-BL), with impulse noise and a time dispersive channel. In each case, various values of the parameter p of the Bernoulli distribution for the impulse noise are considered. The variances of AWGN and impulse noise are equal for $p = 10^{-2}$ only, i.e., $\sigma_w^2 = 10^{-2}\,\sigma_i^2$. The number of MC sub-channels is set to $N = 64$.

value of 3 bits per channel use, the SNR loss for SC schemes is approximately equal to 1.5 dB at $p = 10^{-1}$, and negligible at $p = 10^{-2}$ and $p = 10^{-3}$. As to the interleaved MC case with $N = 64$ and spectral efficiency of 3 bits per channel use, the SNR loss, with respect to the AWGN channel, is 10.6 dB at $p = 10^{-1}$, 4.2 dB at $p = 10^{-2}$, and negligible at $p = 10^{-3}$, respectively. In the presence of a dispersive channel, the behavior of the IR for both SC and interleaved MC schemes confirms the previous analysis, i.e., for a fixed value of the Bernoulli parameter p, the SNR penalty incurred by the interleaved MC scheme is clearly larger than that incurred by the SC scheme.

Moreover, from the results in Fig. 6, one can observe that the SNR loss associated with a MC scheme is always larger than that of a SC scheme, unless at very high rates and limited dispersion (see Fig. 5). Finally, under the condition of no impulse noise (i.e., $p = 0$), the IR curves in Fig. 6 confirm a well-known result: at high code rates, MC schemes with uniform power loading are unable to effectively cope with a dispersive channel. Optimal allocation of the transmitter power (water-filling) and bit loading over the subcarriers [9], [10], [12], is then required.

In Fig. 7, the impact of water-filling power and bit loading techniques on the IR of MC schemes is analyzed, considering the channel in Fig. 6. For uniform power loading, the energy normalization of the channel impulse response implies that E_s also represents the transmitted symbol energy. This is not the case for non-uniform power loading, such as that entailed by the water filling solution, which is known to maximize the information rate under a transmit power constraint. As a consequence, Fig. 7 uses a peculiar definition of E_s as the average transmit symbol energy. A comparison between SC schemes and MC schemes with water-filling and bit-loading is also considered in [21], [22]. The water-filling spectral shaping of the transmitted signal is performed as in standard MC schemes subject to AWGN. The bit loading algorithm in [44], designed to maximize the overall IR with a given input set cardinality, is considered. In other words, the average number of bits per sub-carrier constellation is fixed to 4, corresponding to the number of bits of an (average) 16 QAM modulation format. This bit-loading algorithm (i) ensures that the IR saturates at 4 bits per channel use at high values of SNR, thus allowing effective comparison with fixed 16 QAM schemes, and (ii) guarantees that the number of bits transmitted for each MC symbol is fixed. The variances of impulse noise and AWGN are such that $\sigma_w^2 = 10^{-2}\sigma_i^2$. From Fig. 7, one can observe that the use of water-filling spectral shaping and bit-loading techniques allows to completely recover the gap between MC and SC schemes for small values of the impulse noise power and p (i.e., $p \leq 10^{-3}$). On the other hand, it is easily recognized that for sufficiently large values of impulse noise power and p (e.g., $p \geq 10^{-2}$), MC schemes incur an unavoidable loss, which can be accurately estimated as

$$\text{Loss}_{\text{MC}} = \frac{p\sigma_i^2 + \sigma_w^2}{\sigma_w^2}.$$

In other words, as expected, the MC scheme "converts" the impulse noise into an equivalent AWGN with equal power. In the considered scenario, this leads to a loss of about 3 dB for $p = 10^{-2}$ and about 10 dB for $p = 10^{-1}$.

B. Discussion

We now comment on the obtained results, addressing SC and interleaved MC schemes.

1) SC Schemes: From the results in Fig. 4, it is clear that, even if the impulse noise power equals the AWGN power, the impact of impulse noise on the IR of SC schemes is negligible as long as the occurrence of an impulse noise event is sufficiently rare (i.e., p is sufficiently small).

2) Interleaved MC Schemes: The information-theoretic results, relative to interleaved MC systems, presented in Fig. 4, are obtained assuming an ideal infinite interleaver. These performance results suggest that MC systems, designed assuming

independence of the noise samples affecting different sub-carriers, should exhibit a significant performance loss with respect to SC schemes. For example, under the assumption that the variances of AWGN and impulse noise satisfy the condition $\sigma_w^2 = p\sigma_i^2$, as considered in Fig. 4, the expected SNR penalty of 3 dB has an intuitive explanation. In fact, in the presence of an impulse noise realization, the total noise power in the frequency domain (at the output of the DFT block) doubles.

The penalty affecting MC systems has a different nature with respect to the penalty affecting SC systems. In the SC case, the penalty is "intrinsic", i.e., caused by the introduction of impulse noise, and no coding scheme can overcome it. In the MC case, a portion of this penalty is due to the system design constraints, i.e., transmission of a coded QAM signal designed for a single memoryless channel and distributed over the sub-carriers. In this design practice, the correlation between noise samples in the subcarriers is neglected (this is modeled as ideal interleaving). In principle, in the MC case a significant portion of the penalty due to impulse noise could be recovered by properly accounting for the correlation between noise samples. However, the complexity of this approach increases exponentially with the square of the OFDM block length (all noise samples in the block are correlated).

We remark that the obtained results are confirmed if water-filling spectral shaping and bit-loading are considered, i.e., in all scenarios in which a feedback channel is available such as, e.g., DSL, powerline communications, WiMAX (World-wide interoperability for Microwave Access), next-generation WiFi (Wireless Fidelity), and "fourth generation" (4G) mobile wireless systems [45].

In the following, the obtained IR results will be validated and complemented by a BER-based performance analysis. In general, the IR evaluation does not allow to precisely predict the BER performance, although upper and lower bounds on the BER, based on the IR, can be derived [46], [47]. Nevertheless, the IR provides a limit to the best attainable performance and, therefore, should characterize accurately the BER performance in a scenario where a proper powerful coding scheme is used, as it will be shown in Section IV-B with the use of an LDPC code.

IV. Communication-Theoretic Performance Analysis: Bit Error Rate

In order to validate the prediction of our information-theoretic analysis, we now evaluate, through Monte Carlo simulations, the BER performance of a few SC and MC schemes. More precisely, we first evaluate the performance of TCM schemes, and then we extend our analysis to LDPC-coded schemes.

A. Trellis Coded Modulated Transmission

TCM is a widely used coding/modulation technique for spectrally efficient communication systems [23]–[26]. In this subsection, we derive the exact branch metric to be used in a Viterbi algorithm (VA) in order to perform maximum *a posteriori* (MAP) sequence detection in a SC scheme and in an interleaved MC system with Bernoulli-Gauss impulse noise. The BER performance of TCM schemes is evaluated employing the derived branch metrics along with a modified MC receiver based on a very simple *time-domain processing* suggested by the information-theoretic results.

1) Optimal Branch Metric for SC schemes with Impulse Noise: We define as K the transmission length and denote by $\boldsymbol{a} = \boldsymbol{a}_1^K$ the complex vector corresponding to the information sequence and by $\boldsymbol{r} = \boldsymbol{r}_1^K$ the vector of samples at the output of the channel. According to (1), the observable can be written as $r_k = c_k(a_k, \mu_k) + m_k$, where the TCM symbol $c_k(a_k, \mu_k)$, belonging to a QAM constellation, is a function of the encoder state μ_k and the information symbol a_k at the input of the encoder. Recalling the definition (4) of the PDF for the Bernoulli-Gauss impulse noise and assuming that the information symbols are i.i.d. and equiprobable, the MAP detection strategy can be formulated as

$$\begin{aligned}\hat{\boldsymbol{a}} &= \underset{\boldsymbol{a}}{\operatorname{argmax}} \sum_{k=0}^{K-1} \log\left\{(1-p)\mathcal{N}\left(r_k; c_k(a_k,\mu_k), \sigma_w^2\right)\right. \\ &\quad \left. + p\mathcal{N}\left(r_k; c_k(a_k,\mu_k), \sigma_w^2 + \sigma_i^2\right)\right\}. \end{aligned} \tag{14}$$

Defining the quantities

$$\begin{aligned}\alpha_k(a_k,\mu_k) &\triangleq \frac{1}{2\sigma_w^2}\left\{|r_k - c_k(a_k,\mu_k)|^2\right\} - \ln\left(\frac{1-p}{2\pi\sigma_w^2}\right) \\ \beta_k(a_k,\mu_k) &\triangleq \frac{1}{2(\sigma_w^2+\sigma_i^2)}\left\{|r_k - c_k(a_k,\mu_k)|^2\right\} \\ &\quad - \ln\left(\frac{p}{2\pi(\sigma_w^2+\sigma_i^2)}\right)\end{aligned}$$

one can show that (14) can be rewritten as

$$\begin{aligned}\hat{\boldsymbol{a}} &= \underset{\boldsymbol{a}}{\operatorname{argmin}} \sum_{k=0}^{K-1} \left\{\min[\alpha_k(a_k,\mu_k), \beta_k(a_k,\mu_k)]\right. \\ &\quad \left. - \ln\left(1 + e^{-|\Delta_k(a_k,\mu_k|}\right)\right\} \end{aligned} \tag{15}$$

where $\Delta_k(a_k,\mu_k) \triangleq \alpha_k(a_k,\mu_k) - \beta_k(a_k,\mu_k)$. The branch metric to be used in the VA at epoch k is simply given by the k-th term of (14). The VA-based detection strategy embedded in (15) can now be used to perform sequence detection in SC TCM schemes. We point out that a similar technique is used in [48] to compute the branch metric for a VA, considering different channel and impulse noise models. This indirectly confirms that the theoretical framework proposed in this paper can be extended straightforwardly to scenarios with different models of impulse noise.

2) Optimal Branch Metric for Interleaved MC Schemes with Impulse Noise: In order to derive the branch metric for a MC TCM system, assuming i.i.d. noise samples, one can simply adopt the MAP detection strategy using the noise PDF given by (5). As a consequence, the MAP strategy can be expressed as

$$\hat{\boldsymbol{a}} = \underset{\boldsymbol{a}}{\operatorname{argmax}} \sum_{v=0}^{K-1}\sum_{k=0}^{N-1} \lambda_k(a_k,\mu_k) \tag{16}$$

where K is the number of OFDM symbols, N is the number of carriers per OFDM symbol, and the branch metric is given

by

$$\lambda_k(a_k,\mu_k) = \log\left\{\sum_{\ell=0}^{N}\binom{N}{\ell}p^{\ell}(1-p)^{N-\ell} \cdot\mathcal{N}(r_{k+vN};c_{k+vN}(a_k,\mu_k),\sigma_{\Omega}^2[\ell])\right\} \quad (17)$$

with $\sigma_{\Omega}^2[\ell]$ defined as in (6). Defining

$$\delta_k^{(\ell)}(a_k,\mu_k) \triangleq \frac{1}{2\sigma_{\Omega}^2[\ell]}\left\{|r_{k+vN}-c_{k+vN}(a_k,\mu_k)|^2\right\} - \ln\left\{\binom{N}{\ell}p^{\ell}(1-p)^{N-\ell}\right\} + \ln\left(2\pi\sigma_{\Omega}^2[\ell]\right)$$

where $\ell = 0,1,\ldots,N$, one can express (16) as

$$\hat{\boldsymbol{a}} = \underset{\boldsymbol{a}}{\operatorname{argmin}}\sum_{v=0}^{K-1}\sum_{k=0}^{N-1}\left\{\min[\delta_k^{(0)}(a_k,\mu_k),\bar{\delta}_k^{(1)}(a_k,\mu_k)] - \ln\left(1+e^{-|\bar{\Delta}_k^{(0)}(a_k,\mu_k)|}\right)\right\} \quad (18)$$

where the quantities $\bar{\delta}_k^{(\ell)}(a_k,\mu_k)$ and $\bar{\Delta}_k^{(\ell)}(a_k,\mu_k)$ are recursively defined, for $\ell = 1,\ldots,N-2$ and $\ell = 0,\ldots,N-2$, respectively, as

$$\bar{\delta}_k^{(\ell)}(a_k,\mu_k) \triangleq \min[\delta_k^{(\ell)}(a_k,\mu_k),\bar{\delta}_k^{(\ell+1)}(a_k,\mu_k)] - \ln\left(1+e^{-|\bar{\Delta}_k^{(\ell)}(a_k,\mu_k)|}\right)$$

$$\bar{\Delta}_k^{(\ell)}(a_k,\mu_k) \triangleq \delta_k^{(\ell)}(a_k,\mu_k) - \bar{\delta}_k^{(\ell+1)}(a_k,\mu_k)$$

and, for $\ell = N-1$, as

$$\bar{\delta}_k^{(N-1)}(a_k,\mu_k) \triangleq \min[\delta_k^{(N-1)}(a_k,\mu_k),\delta_k^{(N)}(a_k,\mu_k)] - \ln\left(1+e^{-|\Delta_k^{(N-1)}(a_k,\mu_k)|}\right)$$

with $\Delta_k^{(N-1)}(a_k,\mu_k) \triangleq \delta_k^{(N-1)}(a_k,\mu_k) - \delta_k^{(N)}(a_k,\mu_k)$. Note that (15) can be obtained from (18) for $N = 1$.

While the above branch metrics are optimal for a receiver in an *interleaved* MC scheme, in the following the same metrics and receiver will be used in standard (i.e., non-interleaved) MC schemes, where they are suboptimal. In fact, they do not account for the correlation between noise samples introduced by the DFT block. As it will be shown in the following subsection, the performance obtained using the interleaved MC metric in a (non-interleaved) MC scheme is good and in agreement with the information-theoretic results.

3) Numerical Results: The performance of SC and MC TCM schemes is assessed in terms of BER versus the symbol SNR E_s/N_0 for non-dispersive channels. The considered values for the probability p of occurrence of a noise impulse are 10^{-1} and 10^{-2}.

In Fig. 8, the MC schemes make use of a number of carriers N equal to either 64 or 1024. An eight-state four-dimensional (4D) 64 QAM TCM scheme with rate $\eta = 5.5/6$ and four code bits per 4D symbol is considered [26], and the VA computes the metrics (15) and (18) for SC and MC schemes, respectively. The average power of the impulse noise is kept equal to the power of the AWGN, i.e., $\sigma_w^2 = p\,\sigma_i^2$. As a reference, the theoretical limits for the considered spectral efficiency of 5.5 bits/channel use are shown, for both AWGN and interleaved MC channels, as vertical dotted lines (these values are taken from Fig. 4). As to the BER performance of the SC scheme, one can observe that the presence of a sufficiently rare noise impulse causes an error floor at BER values close to the Bernoulli parameter p, in good agreement with the case of uncoded SC QAM schemes presented in [30]. These results show that TCM schemes are not suitable to cope with impulse noise. This is due to the insufficient protection of the uncoded bits, provided by "set partitioning," against a noise impulse. Moreover, the presence of impulse noise with $p = 10^{-1}$ leads to an SNR loss for MC with $N = 64$ and $N = 1024$ subcarriers, with respect to the AWGN channel, comparable to that predicted by the theoretical analysis. This further confirms the validity of the presented theoretical analysis. However, there is no agreement between theoretical and simulation results for $p < 10^{-1}$ and $N = 64$. This behavior is due to the fact that the average number of impulse noise events, i.e., Np, is larger than 1 for $p = 10^{-1}$, whereas $Np \ll 1$ for $p = 10^{-2}$. Therefore, for small values of p the noise samples after the DFT block exhibit an *impulsive behavior*, limiting the performance of TCM schemes. Note that, by increasing the number of subcarriers N, the BER in the MC case with $p = 10^{-2}$ approaches the BER obtained with $p = 10^{-1}$, in good agreement with the IR results presented in Fig. 4. This is due to the fact that, for a sufficient large value of the number N of subcarriers, $Np \gg 1$.

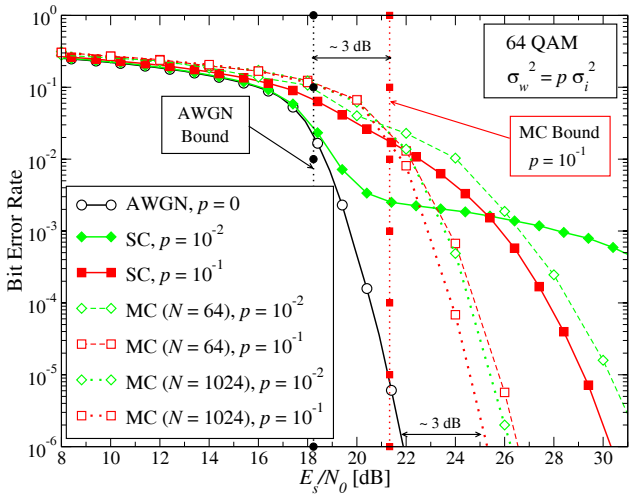

Fig. 8. BER performance in the presence of impulse noise for a 4D-TCM coded 64 QAM SC and MC systems (with $N = 64$ and $N = 1024$). In particular, two possible values for the Bernoulli parameter p are considered. For comparison, the performance in the absence of impulse noise is also shown.

In Fig. 9, the performance of a 16 QAM MC system with the eight-state TCM scheme used in Fig. 8 is shown. The number of sub-carriers is set to $N = 1024$. The BER performance in the presence of Bernoulli-Gauss impulse noise, with parameter $p \in \{10^{-1},10^{-2},10^{-3}\}$ and $\sigma_w^2 = p\,\sigma_i^2$, is analyzed. For comparison, the performance in the absence of impulse noise, i.e., with AWGN, is investigated. In the figure, the theoretical SNR limit predicted by the information-theoretic results for $N = 1024$ and spectral efficiency equal to 3.5 bits/channel use is also shown as vertical lines. Motivated by the theoretical results in Section III, we also consider the use of simple time-

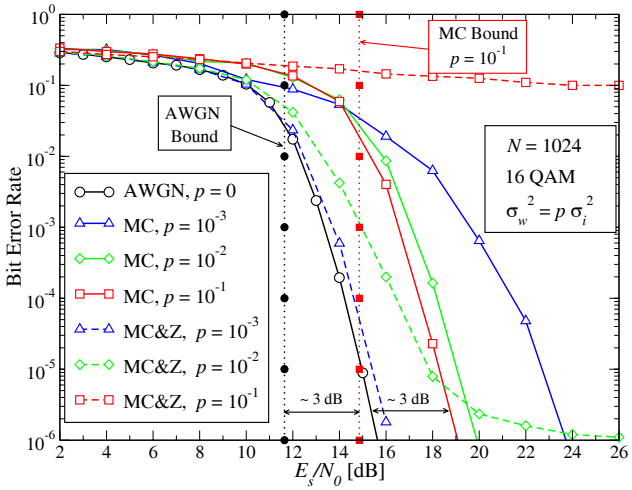

Fig. 9. BER performance in the presence of impulse noise, for a 4D-TCM 16 QAM MC system with $N = 1024$ sub-channels, with and without zeroing of the samples affected by impulse noise. The variances of AWGN and impulse noise are equal for all values of p, i.e., $\sigma_w^2 = p\,\sigma_i^2$. For comparison, the performance in the absence of impulse noise is also shown.

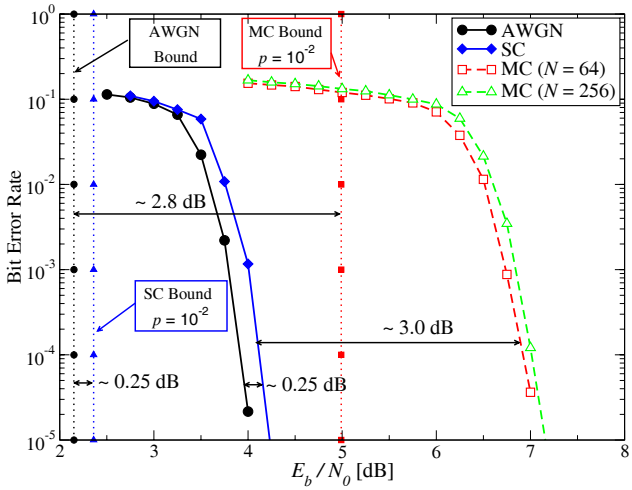

Fig. 10. BER performance, for an LDPC coded 16 QAM, both SC and interleaved MC, over AWGN channel and Bernoulli-Gauss impulse noise channel. The LDPC code is regular (3,6) with codeword length equal to 6000 bits. The Bernoulli parameter is $p = 10^{-2}$ and the noise variances satisfy $\sigma_w^2 = p\,\sigma_i^2$.

domain processing before the DFT. This processor simply detects the presence of strong noise impulses and substitutes them with zeros. A similar approach is considered in [18]. Since the focus of this paper is on a theoretic performance analysis, we assume that the impulse noise detector is ideal, i.e., the noise impulses are perfectly detected (genie-aided detection).[4] The corresponding BER curves are labeled as "MC & Z." Moreover, by considering the BER curves of the system using the proposed time-domain processing, one can conclude that a simple impulse cancellation algorithm can prevent almost completely the loss due to impulse noise, as long as the rate of occurrence of this noise is sufficiently low. We remark that the error floor characterizing these BER curves is due to the fact that signal zeroing does not completely remove the impulse noise, i.e., there is a *residual* noise with magnitude equal to that of the corresponding transmitted signal sample. Note that the use of impulse noise cancellation techniques has been used also in [49], [50].

B. LDPC-Coded Transmission

In this section, the performance of LDPC-coded modulation with 16 QAM is investigated considering three different transmission schemes over non-dispersive channels: (i) a SC scheme with AWGN (and *no* impulse noise), (ii) a SC scheme with Bernoulli-Gauss impulse noise, and (iii) a MC scheme with Bernoulli-Gauss impulse noise. The transmitter collects information bits into vectors of length k, which are LDPC-encoded into a vector of binary symbols of length n (i.e., the codeword). The codeword binary symbols are then grouped into 4-tuples and fed to the modulator, which performs Gray mapping of the bits into 16 QAM symbols. At the receiver, a 16 QAM soft demapper computes the a posteriori probability (APP) of each component bit of the 16 QAM symbol on the basis of the constellation structure and the noise PDF. The APPs are fed to the LDPC decoder, which in turn decodes the codeword by a Gallager soft-output algorithm [27], [51].

The scheme described in the previous paragraph can also be interpreted as a particular instance of a BICM scheme [14], where the interleaver has been omitted due to the random structure of the LDPC code. The use of BICM techniques allows to treat the modulator-channel-demodulator cascade as a memoryless channel. Since the performance of LDPC-coded schemes over memoryless channels depend almost only on the IR of the channel [52], we expect that the performance of the proposed LDPC-coded scheme over the considered channels will behave as predicted by the IR results in Fig 4.

In Fig. 10, the performance of a regular (3,6) LDPC code [28], mapped over a 16 QAM constellation and transmitted over the three considered channels, is shown as a function of the bit SNR E_b/N_0, with E_b being the received energy per information bit. The codeword length is 6000. The maximum number of iterations is set to 100—if the decoder finds a codeword before the 100-th iteration, it stops. The parameter of the Bernoulli-Gauss impulse noise is $p = 10^{-2}$, and the power of the impulse noise equals the power of the AWGN, i.e., $\sigma_w^2 = p\,\sigma_i^2$. The MC schemes make use of a number of carriers N equal to either 64 or 256. As a reference, the theoretical SNR limits for a spectral efficiency of 2 bits per channel use are shown as vertical lines for (i) the SC scheme with AWGN, (ii) the SC scheme with impulse noise, and (iii) the MC scheme with impulse noise. The performance gap, in terms of SNR, between the SC scheme with AWGN and the SC scheme with impulse noise is about 0.25 dB, whereas the gap between the SC scheme with AWGN and the interleaved MC scheme with impulse noise is approximately 3 dB. These results are in excellent agreement with the theoretical limits predicted in Fig. 4.

V. Concluding Remarks

In this paper, the ultimate performance limits of communication schemes affected by impulse noise have been

[4]Detection of a bit interval affected by an impulse of noise can be easily implemented in practice by means of a proper threshold detector.

investigated. The presence of impulse noise has been taken into account through a Bernoulli-Gauss noise model. The analysis has been carried out from an information-theoretic viewpoint, by evaluating the IR of SC and MC schemes. The obtained information-theoretic results suggest that standard MC schemes, operating at coding rates of practical interest, "intrinsically" suffer from a degradation, in terms of maximum achievable IR, with respect to SC schemes. In order to validate these theoretical conclusions, we have evaluated the BER performance of several coded-modulation schemes (both TCM and LDPC-coded): the obtained results are in excellent agreement with the theoretical predictions.

REFERENCES

[1] J. Häring and A. J. H. Vinck, "Coding for impulsive noise channels," in *Proc. Int. Symp. Power-Line Commun. its Apps. (ISPLC'01)*, Malmö, Sweden, Apr. 2001, pp. 103-108.

[2] H. Nakagawa, D. Umehara, S. Denno, and Y. Morihiro, "A decoding for low density parity check codes over impulsive noise channels," in *Proc. Int. Symp. Power-Line Commun. and its Apps. (ISPLC'05)*, Vancouver, Canada, Apr. 2005, pp. 85-89.

[3] H. Meng, Y. L. Guan, and S. Chen, "Modeling and analysis of noise effects on broadband power-line communications," *IEEE Trans. Power Delivery*, vol. 20, no. 2, pp. 630-637, Apr. 2005.

[4] K. J. Kerpez and A. M. Gottlieb, "The error performance of digital subscriber lines in the presence of impulse noise," *IEEE Trans. Commun.*, vol. 43, no. 5, pp. 1902-1905, May 1995.

[5] N. Nedev, S. McLaughlin, D. Laurenson, and R. Daley, "Data errors in ADSL and SHDSL systems due to impulse noise," in *Proc. IEEE Int. Conf. Acoustics, Speech, Signal Processing (ICASSP '02)*, vol. 4, Orlando, Florida, USA, May 2002, pp. 4048-4051.

[6] K. L. Blackardand, T. S. Rappaport, and C. W. Bostian, "Measurements and models of radio frequency impulsive noise for indoor wireless communications," *IEEE J. Select. Areas Commun.*, vol. 11, no. 7, pp. 991-1001, Sept. 1993.

[7] B. Hirosaki, "An orthogonally multiplexed QAM system using the discrete Fourier transform," *IEEE Trans. Commun.*, vol. 29, no. 6, pp. 982-989, July 1981.

[8] I. Kalet, "The multitone channel," *IEEE Trans. Commun.*, vol. 37, no. 2, pp. 119-124, Feb. 1989.

[9] J. A. C. Bingham, "Multicarrier modulation for data transmission: an idea whose time has come," *IEEE Commun. Mag.*, vol. 28, no. 5, pp. 5-14, May 1990.

[10] H. Sari, G. Karam, and I. Jeancleade, "Transmission techniques for digital terrestrial TV broadcasting," *IEEE Commun. Mag.*, vol. 33, no. 2, pp. 100-109, Feb. 1995.

[11] J. A. C. Bingham, *ADSL, VDSL, and Multicarrier Modulation*. New York: John Wiley & Sons, 1997.

[12] M. Engels, *Wireless OFDM Systems: How to Make Them Work?* Springer-Verlag, 2002, M. Engels ed.

[13] M. Ardakani, F. R. Kschischang, and W. Yu, "Low-density parity-check coding for impulse noise correction on power-line channels," in *Proc. Int. Symp. Power-Line Commun. Its Apps. (ISPLC'05)*, Vancouver, Canada, Apr. 2005, pp. 90-94.

[14] G. Caire, G. Taricco, and E. Biglieri, "Bit-interleaved coded modulation," *IEEE Trans. Inform. Theory*, vol. 44, no. 3, pp. 927-946, May 1998.

[15] D. Middleton, "Statistical-physical models of electromagnetic interference," *IEEE Trans. Electromagn. Compat.*, vol. 19, no. 3, pp. 106-127, Aug. 1977.

[16] A. D. Spaulding and D. Middleton, "Optimum reception in the impulsive interference environment–part I: coherent detection," *IEEE Trans. Commun.*, vol. 25, no. 9, pp. 910-923, Sept. 1977.

[17] D. Middleton, "Procedure for determining the parameters of a first-order canonical models of class A and class B electromagnetic interference," *IEEE Trans. Electromagn. Compat.*, vol. 21, no. 3, pp. 190-208, Aug. 1979.

[18] H. M. Oh, Y. J. Park, S. Choi, J. J. Lee, and K. C. Whang, "Mitigation of performance degradation by impulsive noise in LDPC coded OFDM systems," in *Proc. Int. Symp. Power-Line Commun. its Apps. (ISPLC'06)*, Orlando, Florida, USA, Mar. 2006, pp. 331-336.

[19] J. Häring and A. J. H. Vinck, "OFDM transmission corrupted by impulsive noise," in *Proc. Int. Symp. Power-Line Commun. its Apps. (ISPLC'00)*, Limerick, Ireland, Apr. 2000, pp. 9-14.

[20] T. M. Cover and J. A. Thomas, *Elements of Information Theory*. New York: John Wiley & Sons, 1991.

[21] J. M. Cioffi, "A multicarrier primer," Amati Commun. Corp. Stanford University, Tech. Rep., November 1991, ANSI Contribution T1E1.4/91-157. [Online]. Available: http://www-isl.stanford.edu/ cioffi/pdf/multicarrier.pdf.

[22] ——, *Digital communications*, Stanford Univ., Stanford, CA, USA, course notes EE379A. [Online]. Available: http://www.stanford.edu/class/ee379a/.

[23] G. Ungerboeck, "Channel coding with multilevel/phase signals," *IEEE Trans. Inform. Theory*, vol. 28, no. 1, pp. 55-67, Jan. 1982.

[24] L. F. Wei, "Rotationally invariant convolutional channel coding with expanded signal space–part II: nonlinear codes," *IEEE J. Select. Areas Commun.*, vol. 2, no. 5, pp. 672-686, Sept. 1984.

[25] G. D. Forney, Jr., R. Gallager, G. Lang, F. Longstaff, and S. Qureshi, "Efficient modulation for band-limited channels," *IEEE J. Select. Areas Commun.*, vol. 2, no. 5, pp. 632-647, Sept. 1984.

[26] L. F. Wei, "Trellis coded modulation with multidimensional constellation," *IEEE Trans. Commun.*, vol. IT-33, no. 4, pp. 483-501, July 1987.

[27] R. G. Gallager, *Low-Density Parity-Check Codes*. Cambridge, MA, USA: MIT Press, 1963.

[28] T. Richardson and R. Urbanke, "The capacity of low-density parity-check codes under message passing decoding," *IEEE Trans. Inform. Theory*, vol. 47, no. 2, pp. 599-618, Feb. 2001.

[29] R. Pighi, M. Franceschini, G. Ferrari, and R. Raheli, "Fundamental performance limits for PLC systems impaired by impulse noise," in *Proc. Int. Symp. Power-Line Commun. its Apps. (ISPLC'06)*, Orlando, Florida, USA, Mar. 2006, pp. 277-282.

[30] M. Ghosh, "Analysis of the effect of impulsive noise on multicarrier and single-carrier QAM systems," *IEEE Trans. Commun.*, vol. 44, no. 2, pp. 145-147, Feb. 1996.

[31] D. Arnold and H. A. Loeliger, "On the information rate of binary-input channels with memory," in *Proc. Int. Conf. Communications (ICC'01)*, Helsinki, Finland, June 2001, pp. 2692-2695.

[32] V. Sharma and S. K. Singh, "Entropy and channel capacity in the regenerative setup with applications to Markov channels," in *Proc. IEEE Symposium Inform. Theory (ISIT'01)*, Washington, DC, USA, June 2001, p. 283.

[33] H. D. Pfister, J. B. Soriaga, and P. H. Siegel, "On the achievable information rates of finite state ISI channels," in *Proc. Global Telecommun. Conf. (GLOBECOM'01)*, San Antonio, Texas, USA, Nov. 2001, pp. 2992-2996.

[34] D. Arnold, H. A. Loeliger, P. O. Vontobel, A. Kavcic, and W. Zen, "Simulation-based computation of information rates for channel with memory," *IEEE Trans. Inform. Theory*, vol. 52, no. 8, pp. 3498-3508, Aug. 2006.

[35] E. Biglieri, "Coding and modulation for a horrible channel," *IEEE Commun. Mag.*, vol. 41, no. 5, pp. 92-98, May 2003.

[36] S. A. Kassam, *Signal Detection in Non-Gaussian Noise*. New York: Springer-Verlang, 1988.

[37] T. Oberg and M. Mettiji, "Robust detection in digital communications," *IEEE Trans. Commun.*, vol. 43, no. 5, pp. 1872-1876, May 1995.

[38] X. Wang and H. V. Poor, "Robust multiuser detection in non-Gaussian channels," *IEEE Trans. Signal Processing*, vol. 47, no. 2, pp. 289-305, Feb. 1999.

[39] S. M. Zabin and H. V. Poor, "Parameter estimation for Middleton class A interference processes," *IEEE Trans. Commun.*, vol. 37, no. 10, pp. 1042-1051, Oct. 1989.

[40] M. S. Britton and M. L. Scholz, "A practical utilization of Middleton EMI models: automated modelling, parameter estimation and optimization," *Defence Science and Technology Organisation Technical Report DSTO-TR-0234*, Aug. 1995. [Online]. Available: http://www.dsto.defence.gov.au/publications/2299/DSTO-TR-0234.pdf.

[41] S. Haykin, *Communication Systems*. New York: John Wiley & Sons, 1994.

[42] B. G. Leroux, "Maximum-likelihood estimation for hidden Markov models," *Stoch. Process. Appl.*, vol. 40, pp. 127-143, 1992.

[43] L. R. Bahl, J. Coke, F. Jelinek, and J. Raviv, "Optimal decoding of linear codes for minimizing symbol error rate," *IEEE Trans. Inform. Theory*, vol. 20, no. 3, pp. 284-287, Mar. 1974.

[44] M. Franceschini, R. Pighi, G. Ferrari, and R. Raheli, "From information rate computation to communication system design," in *Proc. Inform. Theory Workshop its Appl. (ITA'07)*, San Diego, California, USA, Feb. 2007.

[45] S. Hara and R. Prasad, *Multicarrier Techniques for 4G Mobile Communications*. Artech House, 2003.

[46] M. Feder and N. Merhav, "Relations between entropy and error probability," *IEEE Trans. Inform. Theory*, vol. 40, no. 1, pp. 259-266, Jan. 1994.

[47] M. Franceschini, G. Ferrari, and R. Raheli, "LDPC-coded modulations: performance bounds and a novel design criterion," in *Proc. Intern. Symp. Turbo Codes & Relat. Topics*, Munich, Germany, Apr. 2006, paper no. 148.
[48] S. Miyamoto, M. Katayama, and N. Morinaga, "Optimum detection and design of TCM signals under impulsive noise environment," in *Proc. Int. Conf. Syst. Eng. (ICSE'92)*, Melbourne, Australia, Sept. 1992, pp. 473-478.
[49] M. Sliskovic, "Signal processing algorithm for OFDM channel with impulse noise," in *Proc. Int. Conf. Electronics, Circuits Syst. (ICECS'00)*, vol. 1, Lebanon, Dec. 2000, pp. 222-225.
[50] F. Abdelkefi, P. Duhamel, and F. Alberge, "Impulse noise cancellation in multicarrier transmission," *IEEE Trans. Commun.*, vol. 53, no. 1, pp. 94-106, Jan. 2005.
[51] F. R. Kschischang, B. J. Frey, and H.-A. Loeliger, "Factor graphs and the sum-product algorithm," *IEEE Trans. Inform. Theory*, vol. 47, no. 2, pp. 498-519, Feb. 2001.
[52] M. Franceschini, G. Ferrari, and R. Raheli, "Does the performance of LDPC codes depend on the channel?" *IEEE Trans. Commun.*, vol. 54, no. 12, pp. 2129-2132, Dec. 2006.

Riccardo Pighi (S'02-M'08) was born in Piacenza, Italy, in November 1976. He received the Dr. Ing. degree ("Laurea" 5-years program) in Communications Engineering from the University of Parma, Parma, Italy, in 2002, and the Ph.D. degree in information technology from the University of Parma in 2006. He held a post doctorate position at the University of Parma from March 2006 to September 2007. Since 2003, he has been involved in the project of a multicarrier system for Power Line Communication (PLC) in collaboration with Selta S.p.A.. His main research interests are in the area of digital communication systems design, adaptive and multirate signal processing, storage systems, information theory, power line communications, DSP and FPGA design.

Dr. Pighi is coauthor of the paper "Multidimensional Signal Processing and Detection for Storage Systems With Data Dependent Transition Noise" which received the "2006 Best Student Paper Award in Signal Processing and Coding for Data Storage" from the IEEE Communications Society in November 2007. Dr. Pighi served on the Technical Program Committee of the IEEE Global Communications Conference (GLOBECOM 2008), New Orleans, U.S.A. and IEEE International Symposium on Power-Line Communications and Its Applications (ISPLC 2007), Pisa, Italy.

He joined the research staff at Selta, Roveleto di Cadeo, Piacenza in September 2007.

Michele Fransceschini (S'02) was born in Milan, Italy, in 1977. He received the Dr. Ing. degree ("Laurea" 5-year program) in Electrical Engineering (summa cum laude) from the University of Parma in 2002. In 2003, he received the "Paolo Conti Award" as the best graduate in Information Engineering at the University of Parma in the academic year 2002. In 2006, he received the Ph.D. from the University of Parma. From March 2006 to March 2008 he held a postdoc position at University of Parma. He is currently with the IBM T. J. Watson Research Center.

His research interests lie in the area of communication and information theory, with particular emphasis on low density parity check code design, theoretical aspects of optical communication, advanced signal processing techniques, synchronization, and low-complexity implementation of digital communication systems.

Gianluigi Ferrari (S'97-M'03) was born in Parma, Italy, in November 1974. He received the "Laurea" degree (five-year program) (summa cum laude) and the Ph.D. degree in electrical engineering from the University of Parma in October 1998 and January 2002, respectively. From July 2000 to December 2001, he was a Visiting Scholar at the Communication Sciences Institute, University of Southern California, Los Angeles. Since 2002, he has been a Research Professor with the Department of Information Engineering, University of Parma, where he is now the coordinator of the Wireless Ad-hoc and Sensor Networks (WASN) Laboratory. Between 2002 and 2004, he visited several times, as a Research Associate, the Electrical and Computer Engineering Department at Carnegie Mellon University, Pittsburgh, PA.

He has published more than 90 papers in leading international conferences and journals. He is coauthor of a few books, among which *Detection Algorithms for Wireless Communications, with Applications to Wired and Storage Systems* (Wiley: 2004) and *Ad Hoc Wireless Networks: A Communication-Theoretic Perspective* (Wiley: 2006). He is listed in Marquis *Who's Who in the World*, *Who's Who inScience and Engineering*, *Who's Who of Emerging Leaders*, Madison *Who's Who*, and *IBC 2000 Outstanding Intellectuals of the 21st Century*.

His main research interests include wireless ad hoc and sensor networking, and adaptive signal processing. Dr. Ferrari is a co-recipient of a best student paper award at the 2006 International Workshop on Wireless Ad hoc Networks (IWWAN'06). He acts as a technical program member for several international conferences, and also as a frequent reviewer for many international journals and conferences. Since 2007, he has been on the Editorial Board of THE OPEN ELECTRICAL AND ELECTRONIC ENGINEERING JOURNAL (Bentham Publishers) and the INTERNATIONAL JOURNAL OF RF TECHNOLOGIES: RESEARCH AND APPLICATIONS (Taylor & Francis).

Riccardo Raheli (M'87) received the Dr. Ing. (Laurea) degree in Electrical Engineering "summa cum laude" from the University of Pisa, Italy, in 1983, the Master of Science (M.S.) degree in Electrical and Computer Engineering from the University of Massachusetts at Amherst, U.S.A., in 1986, and the Doctoral (Perfezionamento) degree in Electrical Engineering "summa cum laude" from the Scuola Superiore S. Anna di Studi Universitari e di Perfezionamento, Pisa, Italy, in 1987.

From 1986 to 1988 he was with Siemens Telecomunicazioni, Milan, Italy. From 1988 to 1991, he was a Research Professor at the Scuola Superiore S. Anna, Pisa, Italy. In 1990, he was a Visiting Assistant Professor at the University of Southern California, Los Angeles, U.S.A.. Since 1991, he has been with the University of Parma, Italy, first as a Research Professor, then Associate Professor and currently Professor of Communications Engineering and Chairman of the Communications Engineering Program Committee. His scientific interests are in the general area of statistical communication theory, with application to wireless, wired and storage systems, and special attention to data detection in uncertain environments, iterative information processing and adaptive algorithms for communications. His research work has lead to numerous scientific publications in leading international journals and conference proceedings, as well as a few industrial patents. In 1990, he conceived (with Andreas Polydoros) the principle of "Per-Survivor Processing." He is coauthor of the book *Detection Algorithms for Wireless Communications, with Applications to Wired and Storage Systems* (John Wiley & Sons, 2004). He is coauthor of the paper which received the "2006 Best Student Paper Award in Signal Processing & Coding for Data Storage" from the IEEE Communications Society.

Dr. Raheli served on the Editorial Board of the IEEE TRANSACTIONS ON COMMUNICATIONS, as an Editor for Detection, Equalization and Coding, from 1999 to 2003. He was the leading Guest Editor of a special issue of the IEEE JOURNAL ON SELECTED AREAS IN COMMUNICATIONS on "Differential and Noncoherent Wireless Communications," published in 2005. He served on the Editorial Board of the EUROPEAN TRANSACTIONS ON TELECOMMUNICATIONS, as an Editor for Communication Theory, from 2003 to 2008. He has also served on the Technical Program Committee of many leading international conferences in the areas of Communication Theory and Systems, Information Theory and Signal Processing, such as the IEEE International Conference on Communications (ICC), IEEE Global Communications Conference (GLOBECOM), European Signal Processing Conference (EUSIPCO), IEEE International Symposium on Power-Line Communications and Its Applications (ISPLC), International Symposium on Information Theory and its Applications (ISITA), International Symposium on Spread Spectrum Techniques and Applications (ISSSTA), and others.